

*Edoardo Brunson*

**Argonne National Laboratory**

**EBR-II DRY CRITICAL EXPERIMENTS**

**Experimental Results**

by

**R. L. McVean, G. S. Brunson,  
B. C. Cerutti, W. B. Loewenstein,  
F. W. Thalgott, and G. K. Whitham**

## LEGAL NOTICE

*This report was prepared as an account of Government sponsored work. Neither the United States, nor the Commission, nor any person acting on behalf of the Commission:*

- A. Makes any warranty or representation, expressed or implied, with respect to the accuracy, completeness, or usefulness of the information contained in this report, or that the use of any information, apparatus, method, or process disclosed in this report may not infringe privately owned rights; or*
- B. Assumes any liabilities with respect to the use of, or for damages resulting from the use of any information, apparatus, method, or process disclosed in this report.*

*As used in the above, "person acting on behalf of the Commission" includes any employee or contractor of the Commission, or employee of such contractor, to the extent that such employee or contractor of the Commission, or employee of such contractor prepares, disseminates, or provides access to, any information pursuant to his employment or contract with the Commission, or his employment with such contractor.*

ARGONNE NATIONAL LABORATORY  
9700 South Cass Avenue  
Argonne, Illinois

EBR-II DRY CRITICAL EXPERIMENTS

Experimental Results

by

R. L. McVean,\* G. S. Brunson,\*  
B. C. Cerutti,\* W. B. Loewenstein,\*\*  
F. W. Thalgott,\* and G. K. Whitham\*

\*Idaho Division

\*\*Reactor Engineering Division

February 1962





## TABLE OF CONTENTS

	<u>Page</u>
ABSTRACT . . . . .	5
I. INTRODUCTION. . . . .	5
II. DESCRIPTION OF THE EBR-II. . . . .	6
III. EXPERIMENTAL RESULTS. . . . .	13
A. Neutron Source and Instrument Response . . . . .	13
1. Instrumentation . . . . .	14
2. Neutron Source . . . . .	15
3. Instrument Response. . . . .	15
B. The Critical Approach. . . . .	16
1. Condition of Reactor Prior to Critical Approach . . . .	16
2. Loading to Criticality . . . . .	16
C. Reactivity Effects. . . . .	23
1. Control and Safety Rods. . . . .	23
2. Temperature Coefficient of Reactivity . . . . .	26
3. Static Calibration of Oscillator Rod. . . . .	26
4. Replacement Worth of Fuel Subassemblies . . . . .	29
D. Neutron Flux Measurements. . . . .	29
1. Fission and Capture Distributions in the Outer Blanket. . . . .	29
2. Fission Distributions in the Inner Blanket. . . . .	29
3. Leakage Neutron Flux. . . . .	35
E. Power Calibration . . . . .	36
F. Determination of Clean Critical Mass . . . . .	36
G. Wet Critical Instrument Configuration . . . . .	36
IV. SUMMARY . . . . .	37
ACKNOWLEDGMENTS . . . . .	39
REFERENCES. . . . .	39



## LIST OF FIGURES

<u>No.</u>	<u>Title</u>	<u>Page</u>
1.	EBR-II Facility . . . . .	6
2.	EBR-II Reactor Plant . . . . .	7
3.	EBR-II Primary System . . . . .	8
4.	EBR-II Reactor (Vertical Section) . . . . .	9
5a.	EBR-II Reactor (Horizontal Section) . . . . .	10
5b.	Subassembly Loading Diagram . . . . .	11
6.	EBR-II Fuel Handling System . . . . .	12
7.	Nuclear Instrument Thimbles . . . . .	13
8.	Condition of Reactor Prior to Critical Approach . . . . .	14
9.	Approach to Critical - Inverse Count Rate Curves . . . . .	18
10.	Approach to Critical - Inverse Count Rate Curves . . . . .	19
11.	Approach to Critical - Inverse Count Rate Curves . . . . .	19
12.	Approach to Critical - Loading No. 2 . . . . .	20
13.	Approach to Critical - Loading No. 3 . . . . .	20
14.	Approach to Critical - Loading No. 4 . . . . .	20
15.	Approach to Critical - Loading No. 5 . . . . .	20
16.	Approach to Critical - Loading No. 6 . . . . .	21
17.	Approach to Critical - Loading No. 7 . . . . .	21
18.	Approach to Critical - Loading No. 8 . . . . .	21
19.	Approach to Critical - Loading No. 9 . . . . .	22
20.	Approach to Critical - Loading No. 10 . . . . .	22
21.	Approach to Critical - Final Loading No. 11 . . . . .	22
22.	Core Configuration for Most Control and Safety Rod Measurements . . . . .	25
23.	Core Configuration for Reactivity Worth Determination. . . . .	25
24.	Control Rod Calibrations . . . . .	25
25.	Dry Critical Oscillator Rod . . . . .	27
26.	Core Configuration for Oscillator Rod Calibration . . . . .	27

## LIST OF FIGURES

<u>No.</u>	<u>Title</u>	<u>Page</u>
27.	Oscillator Rod Calibration Curves . . . . .	28
28.	Oscillator Rod Boron Carbide Capsule . . . . .	28
29.	Corrected Worth of $B_4^{10}C$ in Oscillator Rod . . . . .	28
30.	Foil Locations for Flux Measurements in Outer Blanket . . . .	30
31.	Core Configuration for Foil Irradiations in 7-C-4 and 7-D-1 .	32
32.	Highly Enriched Uranium Foil Activations in 7-C-4 and 7-D-1 . . . . .	32
33.	Depleted Uranium Foil Activations in 7-C-4 and 7-D-1 . . . .	33
34.	Core Configuration for Foil Irradiations in 6-C-4 and 7-F-5 .	33
35.	Highly Enriched Uranium Foil Activations in 6-C-4 and 7-F-5 . . . . .	34
36.	Depleted Uranium Foil Activations in 6-C-4 and 7-F-5 . . . .	34

## LIST OF TABLES

<u>No.</u>	<u>Title</u>	<u>Page</u>
I.	Count Rates Prior to Critical Approach . . . . .	15
II.	Fuel Subassembly Loading Increments . . . . .	17
III.	Subcritical Multiplication Count Rates . . . . .	17
IV.	Source Decay Correction Factors . . . . .	18
V.	Reactivity Worths of Control and Safety Rods . . . . .	24
VI.	$U^{235}$ and $U^{238}$ Fission and $U^{238}$ Capture Analysis of Foil Set I Irradiated in Outer Blanket . . . . .	30
VII.	$U^{235}$ and $U^{238}$ Fission and $U^{238}$ Capture Analysis of Foil Set II Irradiated in Outer Blanket . . . . .	31
VIII.	$U^{235}$ and $U^{238}$ Fission and $U^{238}$ Capture Analysis of Foil Set III Irradiated in Outer Blanket . . . . .	31
IX.	$U^{235}$ and $U^{238}$ Fission and $U^{238}$ Capture Analysis of Foils Irradiated in Inner Blanket . . . . .	35
X.	Leakage Neutron Flux Measurements . . . . .	35
XI.	Wet Critical Instrument Configuration . . . . .	37



## EBR-II DRY CRITICAL EXPERIMENTS

### Experimental Results

by

R. L. McVean, G. S. Brunson,  
B. C. Cerutti, W. B. Loewenstein,  
F. W. Thalgott, and G. K. Whitham

### ABSTRACT

These experiments are preoperational zero-power nuclear investigations in the Experimental Breeder Reactor II (EBR-II) prior to insertion of sodium coolant. The experiments were performed with the power reactor instruments, fuel and mechanical components installed. The measured dry critical size, reactivity worth of control mechanisms and isothermal temperature coefficient of reactivity are in good agreement with predicted values. Additional measurements include neutron flux distributions in the uranium reflector and outside the reactor neutron shield.

### I. INTRODUCTION

The Experimental Breeder Reactor II (EBR-II) Dry Critical Experiments were conducted prior to filling the reactor system with sodium coolant. The Dry Critical Experiments were performed in accordance with a written, preplanned program.<sup>(1)</sup> A more detailed description of the EBR-II reactor and its associated systems is given in the EBR-II Hazards Summary Report.<sup>(2)</sup> The absence of coolant required that the reactor power level be maintained at less than 1 kw. The low power level prevented the buildup of fission products and plutonium in the fissionable and fertile materials.

The Critical Experiments had two general objectives:

(1) To obtain information relating to the performance of the reactor system without sodium coolant. When compared with future information derived with sodium coolant, it will be possible to determine various sodium effects on the neutronics of the system.

(2) To determine and/or verify certain operational data for later modification or improvement of the system (neutron shield, instrumentation, etc.) before filling the reactor with sodium.

## II. DESCRIPTION OF THE EBR-II

The EBR-II power plant complex (Fig. 1) is located at the United States Atomic Energy Commission National Reactor Testing Station and the plant includes a complete, remotely-operated fuel-processing and fuel-element fabrication facility. It will be the first reactor in the United States Power Reactor Demonstration Program to operate on a closed fuel cycle. Partly spent or burned fuel can be pyrometallurgically reprocessed, re-enriched, and returned to the reactor after being refabricated.

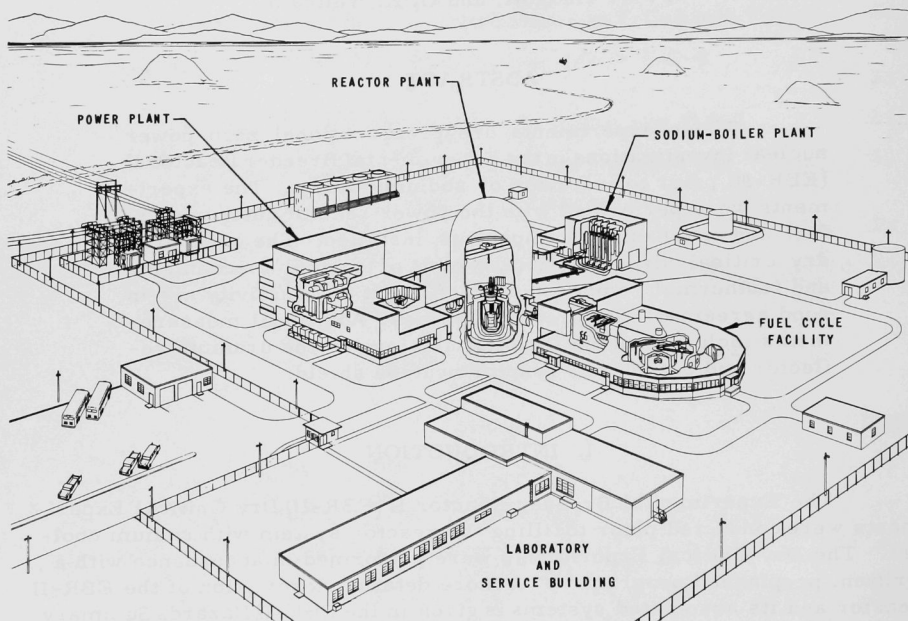


Fig. 1. EBR-II Facility

The reactor is submerged in the primary tank (Fig. 2), containing about 90,000 gal of liquid sodium at  $370^{\circ}\text{C}$ . With a 9000-gpm maximum rate of coolant flow in the reactor, the large sodium reservoir insures that temperature transients in the bulk coolant are very slowly transmitted to the reactor. The large sodium reservoir also serves as a partial sink in case of an accidental energy release. The primary tank is suspended inside an airtight containment building (Figs. 2 and 3) which confines an accidental release of fission products, plutonium, and activated sodium from the primary system.

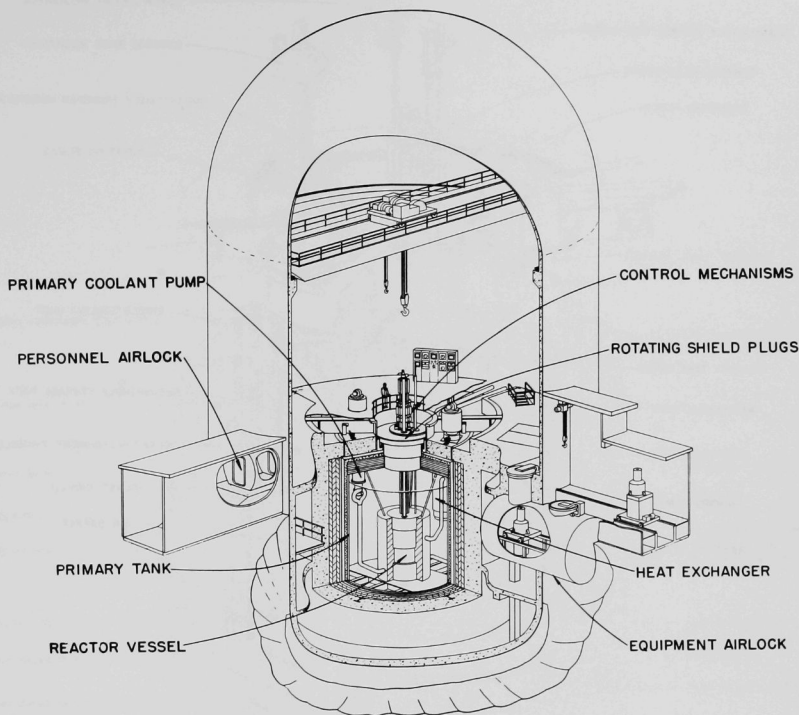


Fig. 2. EBR-II Reactor Plant

The structure of the primary system is designed to contain the energy release associated with a nuclear accident, while the reactor building is designed to confine the effects of a maximum sodium-air interaction caused by a major sodium release. In a sense, the reactor is thus doubly contained.

The reactor is in the reactor vessel near the bottom of the primary tank (Fig. 3). Coolant is taken from the bulk sodium in the primary tank, passed through two 5000-gpm mechanical pumps, and is introduced near the bottom of the reactor vessel. Flow is then upward through individual fuel and breeder-reflector subassemblies. In order to achieve nearly uniform temperatures of the coolant at the outlet, the coolant flow is orificed in a manner consistent with axial and radial power density gradients and discontinuities. The hot ( $482^{\circ}\text{C}$ ) coolant leaves the reactor near the top of the reactor vessel and then passes through the primary heat exchanger submerged in the primary sodium. Sodium is the working fluid of the intermediate secondary cooling system.

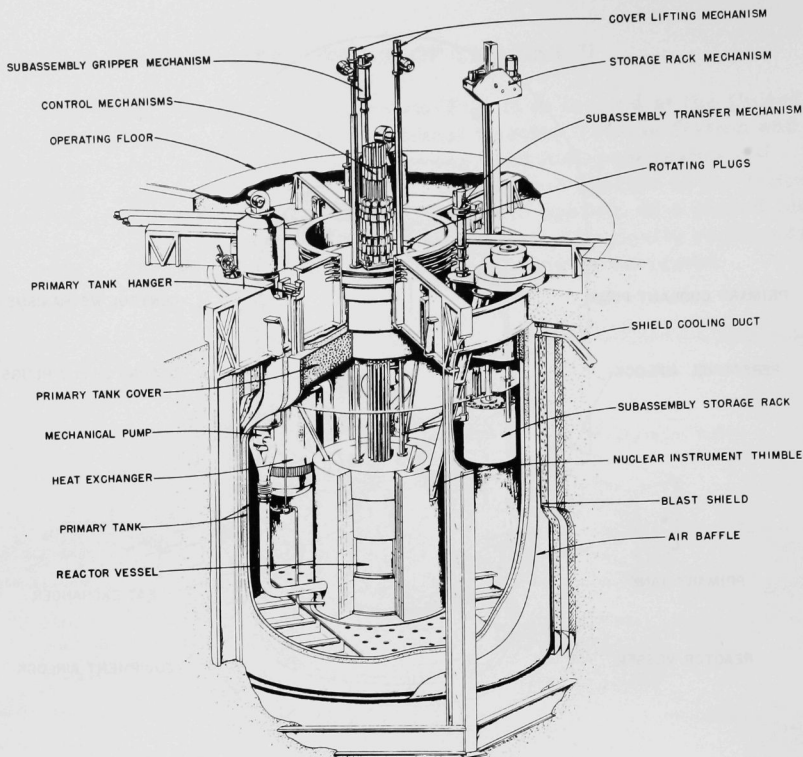


Fig. 3. EBR-II Primary System

Details of the reactor, the surrounding reactor vessel, and the neutron shield are given in Figs. 4 and 5. The reactor (core and breeder reflector) is a hexagonal array of subassemblies (Fig. 5). The subassemblies are mechanically designed to prevent inadvertent interchange between enriched and depleted uranium-bearing subassemblies. Each subassembly contains the fissile or fertile material in the form of cylindrical fuel elements bonded with sodium and clad with stainless steel. The fertile material is unalloyed depleted uranium. The fissile material is contained in uranium-5 w/o fissium fuel alloy. The uranium is 48.4% enriched in  $U^{235}$ . Each fuel subassembly contains 91 fuel elements. Each fuel element contains ~67 g of the uranium-5 w/o fissium alloy for a total of ~2.82 kg of  $U^{235}$  per subassembly.



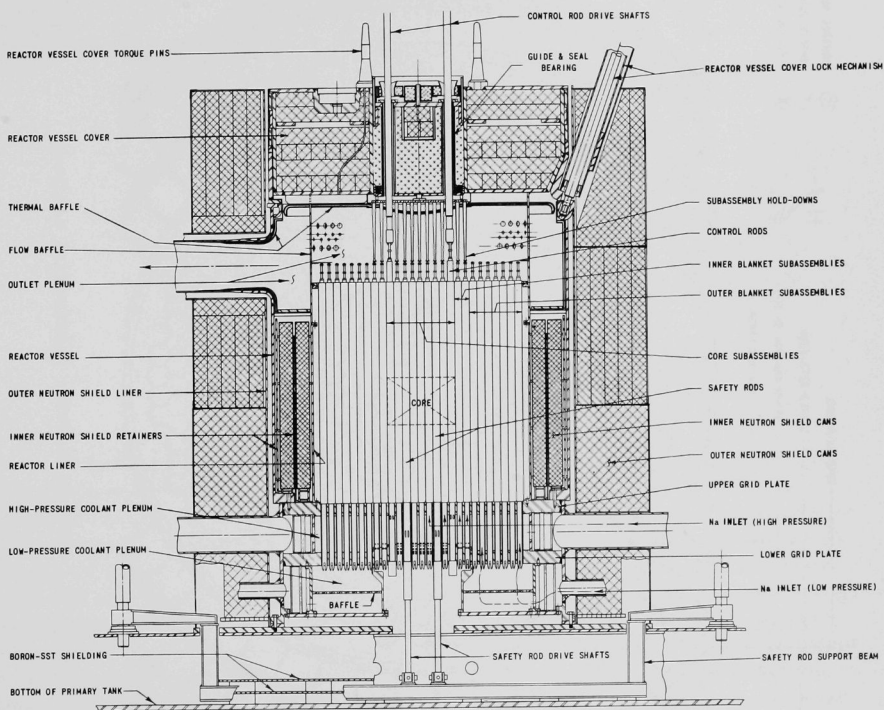


Fig. 4. EBR-II Reactor (vertical section)

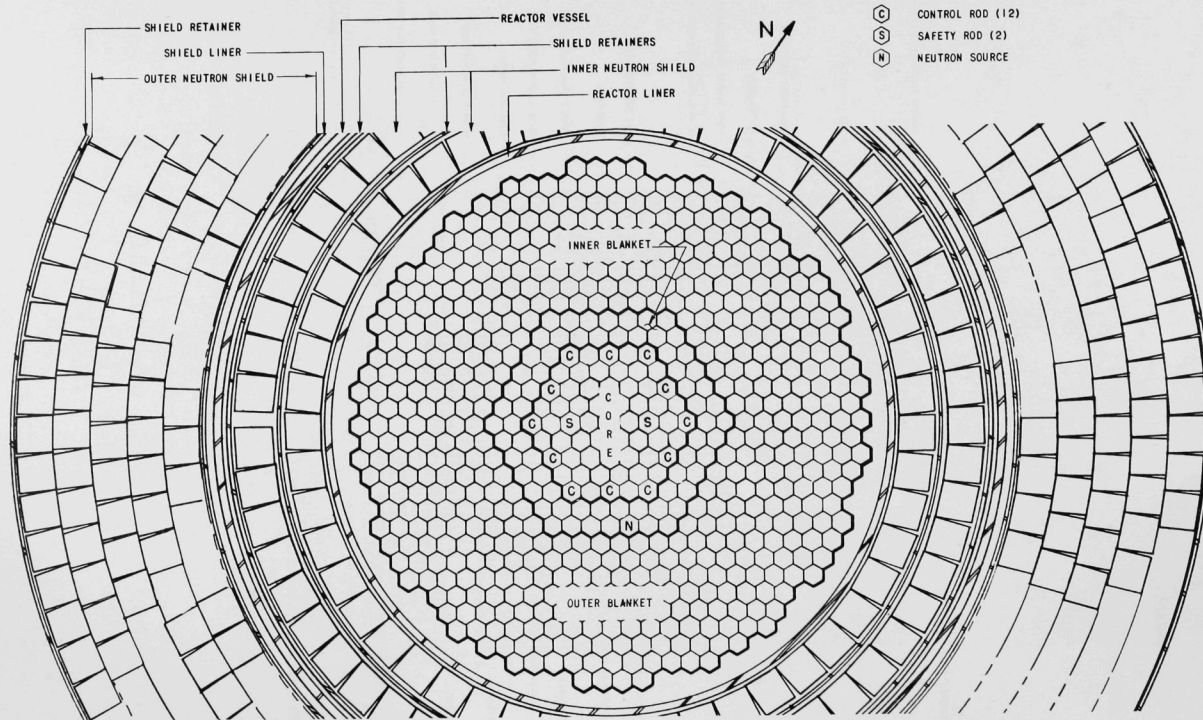


Fig. 5a. EBR-II Reactor (horizontal section)

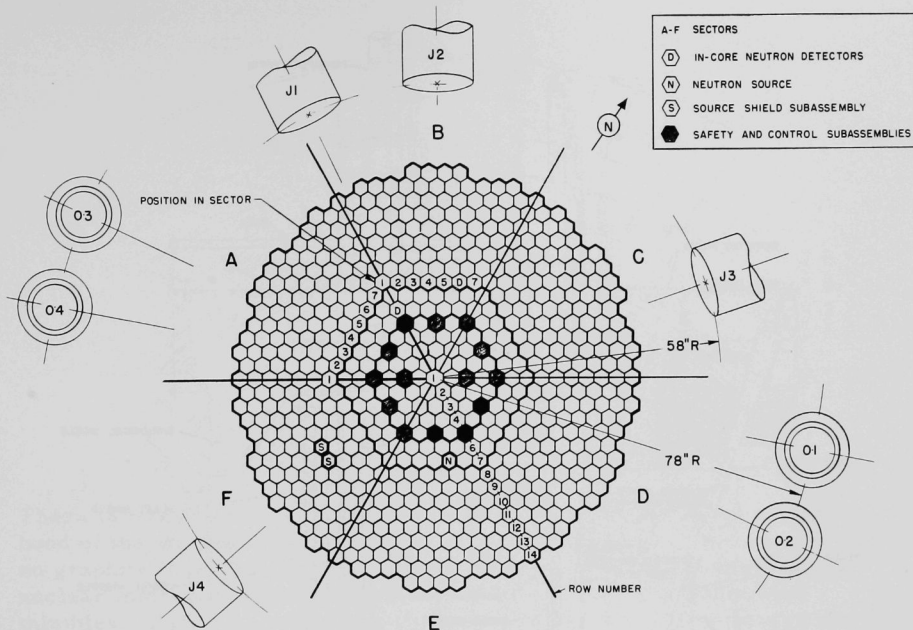


Fig. 5b. Subassembly Loading Diagram

Reactor control is effected by moving fuel into or out of the core from below. There are twelve control and two safety subassemblies. Each of these contains 61 of the same fuel elements used in a normal fuel subassembly. Control and safety rod strokes are 14 in., the approximate length of the core. In the most reactive position, fuel elements in a control rod are at the same elevation as fuel elements in a fuel subassembly. In the least reactive position, the tops of the fuel elements in a control rod are at the same elevation as the bottoms of the fuel elements in a fuel subassembly. The twelve control subassemblies are activated from the top and must be disconnected from their drive mechanisms in their least reactive positions, while fuel is being loaded (Fig. 6). The two safety rods are actuated from below the core (Fig. 4) and are operative while fuel is being loaded. Scram signals actuate these rods depending on the mode of operation. During "Reactor Operation," when the reactor is critical and producing power, an automatic scram signal will release the twelve control rods. With a pressure assist, they move to their least reactive positions. During "Fuel Handling," when the reactor is expected to be substantially subcritical, an automatic scram signal releases the safety rods. Gravity causes them to move to their least reactive positions below the core. The safety rods may also be manually released during "Reactor Operation."

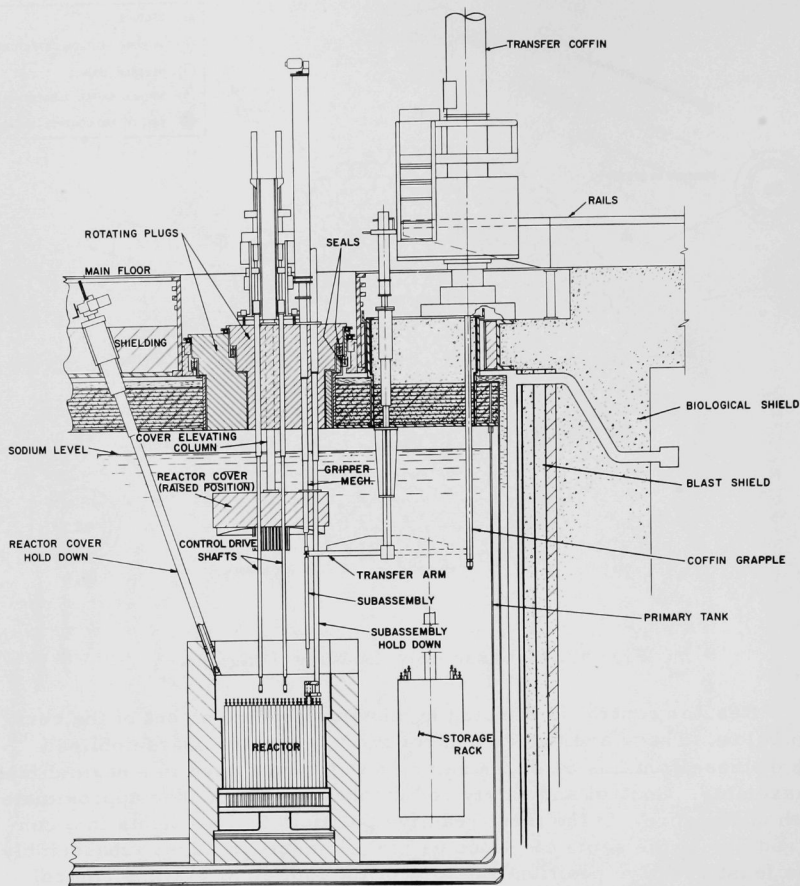


Fig. 6. EBR-II Fuel Handling System

The neutron-flux-monitoring equipment (fission counters and ion chambers) are located in eight air-cooled ( $<45^{\circ}\text{C}$ ) instrument thimbles. Four of these are embedded in the neutron shield surrounding the reactor vessel (Fig. 7). Four more are located in sodium just outside the neutron shield. The fission counters and ion chambers are located near the central plane of the core for maximum sensitivity, but can be moved vertically inside the thimbles. The neutron shield consists mainly of graphite and borated graphite canned in stainless steel. Small amounts of sodium pass between the square shield cans. Borated graphite is used only in those shield regions where it does not interfere with instrument response.



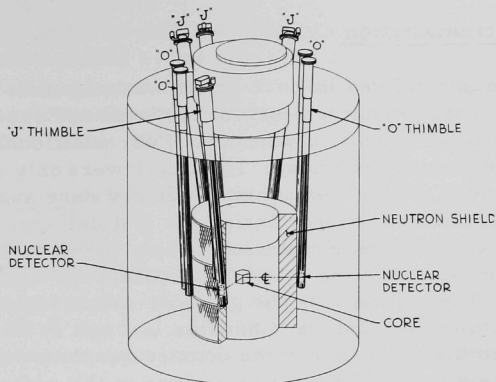


Fig. 7. Nuclear Instrument Thimbles

There is no borated graphite inside the reactor vessel. In the neighborhood of the startup channels ( $J_1$  and  $J_2$  thimbles in Figs. 5 and 7), there is no graphite inside the reactor vessel. There are eleven channels of nuclear instrumentation distributed throughout the eight instrument thimbles. Three log count data channels are operative from source power to about 2 kw. Three log flux and one linear flux channels are operative from 100 watts to full power. Three linear flux channels are operative from 60 kw to full power. One channel is operative from 6 Mw to full power and will be used for automatic control of the reactor at power. Automatic control is not operative until the power level has been manually established.

An Sb-Be neutron source subassembly (Fig. 5b) will be permanently located in the radial blanket of the reactor. The Sb-Be source may be remotely disassembled by reactor fuel-handling equipment. The active Sb rod may be placed in a source shield subassembly located in the outer blanket (Fig. 5b).

### III. EXPERIMENTAL RESULTS

#### A. Neutron Source and Instrument Response

The relationship between the neutron source strength and the neutron detector response was determined during the Dry Critical Experiments. The use of special "in-core" instrumentation provided large counting rates at very low reactor multiplication. Response of the normal instrumentation was simultaneously determined and found to be adequate.

Fig. 8. Condition of Reactor Prior to Critical Approach  
(29.2 kg of  $U^{235}$  loaded)

Since Channels 1, 2 and 3 would have saturated just before criticality, the counting rates were reduced by lowering the amplifier gain and increasing the discriminator voltage prior to the final critical approach. This change in counting rate was considered in listing the corrected subcritical multiplication count rates (Table III).

## (2) Neutron Source

An antimony-beryllium neutron source was located adjacent to the core in position 7-E-3 (Fig. 8). The source had a strength of 270 curies on August 1, 1961, and a half-life of 60 days. The source strength decayed 13% during the critical approach (~2 weeks). All subcritical counts were corrected to a source strength of 189 curies as of September 1, 1961.

## (3) Instrument Response

Count rates were obtained on seven counting channels prior to the critical approach. At that time, the central fuel subassembly with thermocouples, twelve control rods and two safety rods, containing ~29 kg of  $U^{235}$  had been loaded into the core. All other grid plate positions were filled with either fertile or inert material. The special central fuel subassembly contained fourteen thermocouples attached to the cladding of seven fuel elements. These temperatures were recorded in the control room on a multipoint recorder with an alarm set to trip at temperatures greater than 180°F. The counts were obtained on September 18, 1961, with all control and safety rods in the "down" position. Table I gives the count rates obtained with a source strength of 155 curies.

TABLE I. COUNT RATES PRIOR TO CRITICAL APPROACH\*  
(Source Strength ~155 Curies)

Counter	Amplifier Setting		Count Rate (counts/sec)
	Discriminator	Gain	
1	225	1	3.6
2	225	1	3.5
3	250	1	3.1
A	250	1	67.7
B	250	1	43.6
E	150	3	9.6
F	150	16	3.9

\*29.2 kg of  $U^{235}$  loaded in reactor. All control and safety rods in "down" position.

## B. The Critical Approach

A series of steps for loading the fuel subassemblies was proposed by Koch et al.,<sup>(1)</sup> for the critical approach. The actual fuel loading increments were changed after considering the extrapolation of the inverse count rate curves following each loading. These changes were made so that the total fuel in the core, after a proposed loading change, would always be less than the critical mass predicted by the inverse count rate curves after the previous loading.

### (1) Condition of Reactor Prior to Critical Approach

Figure 8 shows the location of the in-core instrument channels, the neutron source, the source storage holes, the control and safety rod positions and the central fuel subassembly with thermocouples. The outer blanket was loaded with depleted uranium blanket subassemblies. The inner blanket, rows 6 and 7, was loaded with depleted uranium inner blanket subassemblies. The core, rows 1 through 5, was loaded with 26 dummy stainless steel subassemblies near the center and 20 natural uranium subassemblies near the boundary. Prior to the critical approach, 15 fuel-bearing subassemblies were also loaded into the core. These were the 12 control rods, 2 safety rods and the special central fuel subassembly. This gave an initial mass of 29.21 kg of  $U^{235}$  in the reactor.\*

### (2) Loading to Criticality

The critical approach began on September 18, 1961. The reactor diverged on a 100-sec period at 7:00 p.m. on September 30, 1961. Table II shows the number of fuel subassemblies added during each of ten incremental fuel loadings. Loading No. 1 includes the fuel-bearing subassemblies loaded prior to the critical approach. Each control and safety subassembly contains approximately 1.89 kg of  $U^{235}$  and each fuel subassembly contains approximately 2.82 kg of  $U^{235}$ .

Subcritical count rates were obtained on all counting channels after each incremental fuel loading.\*\* Counts were obtained with all the control rods out (down) and again when all the control rods were fully inserted (up). In both cases, the safety rods were in the inserted (up) position. Observed count rates were always corrected for source decay. Corrected count rates were used to plot the critical approach curves.

---

\*This does not include the  $U^{235}$  in the fertile materials.

\*\*Count rates were also obtained before and after each fuel subassembly was loaded in addition to startup and shutdown counts at the beginning and end of each day, respectively.



These are graphs of the inverse of the corrected count rates as a function of the number of fuel-bearing subassemblies in the reactor. Table III gives the corrected count rates obtained after each incremental fuel loading. Table IV lists the decay factors used to correct the observed count rates to a constant source strength of 189 curies as of September 1, 1961. Figures 9, 10 and 11 show the inverse count rate curves for seven counting channels.

TABLE II. FUEL SUBASSEMBLY\* LOADING INCREMENTS

Loading No.	Number of Subassemblies Added/Loading	Total Number of Subassemblies	Total Kg of U <sup>235</sup>
1	15*	15	29.21
2	16	31	74.18
3	9	40	99.49
4	9	49	124.98
5	6	55	141.86
6	6	61	158.81
7	6	67	175.73
8	6	73	192.67
9	4	77	203.95
10	6	83	220.88
11	4	87	232.18

\*Including control and safety subassemblies.

TABLE III. SUBCRITICAL MULTIPLICATION COUNT RATES\*

Corrected Counts/Minute†										
Loading No.	Channel 1		Channel 2		Channel 3		Channel A		Channel B	
	C.R. down	C.R. up	C.R. down	C.R. up	C.R. down	C.R. up	C.R. down	C.R. up	C.R. down	C.R. up
1	261	415	254	382	223	332	2,085**	2,380**	3,180	3,860
2	695	857	634	798	565	711	8,760	10,630	5,110	6,420
3	1,061	1,375	972	1,256	867	1,112	12,520	15,850	7,425	9,650
4	1,816	2,460	1,647	2,227	1,505	2,038	19,900	27,120	12,120	16,790
5	2,700	3,915	2,460	3,595	2,250	3,220	28,850	42,150	17,720	26,300
6	4,033	6,620	3,705	6,070	3,385	5,420	41,700	69,000	25,800	43,000
7	6,200	11,260	5,565	10,400	5,135	9,345	59,700	109,700	37,700	69,900
8	11,480	25,600	10,570	23,480	9,560	21,220	104,100	232,800	66,650	150,300
9	15,290	42,600	14,060	39,200	12,610	35,195	132,900	367,000	85,700	238,000
10	23,200	169,700	21,320	154,100	19,320	139,800	194,200	1,321,000	132,600	900,000
11	28,600		25,450		24,550		263,000			

Loading No.	Channel C		Channel D		Channel E		Channel F	
	C.R. down	C.R. up	C.R. down	C.R. up	C.R. down	C.R. up	C.R. down	C.R. up
1	-	-	-	-	697	1,100	283	472
2	-	-	-	-	1,705	2,280	785	1,060
3	-	-	-	-	2,730	3,640	1,268	1,695
4	-	-	-	-	4,680	6,555	2,233	3,120
5	-	-	-	-	7,010	10,500	3,290	5,030
6	-	-	-	-	10,310	17,450	4,958	8,420
7	-	-	-	-	15,600	29,400	7,590	14,300
8	99	231	84	174	27,850	63,900	14,040	32,300
9	138	363	108	293	36,510	103,600	18,600	53,215
10	193	1,410	185	1,200	55,300	398,900	28,200	208,600
11	252		216		76,200		38,800	

\*Count rates corrected to a source strength of ~189 curies as of Sept. 1, 1961, maximum correction is ~40% for Loading No. 11. See Table IV.

\*\*Discriminator setting on Channel A was changed after these counts.

†C.R. down = Control rods down; C.R. up = Control rods up

TABLE IV. SOURCE DECAY CORRECTION FACTORS

(Source Strength ~189 Curies on Sept. 1, 1961)

Loading No.	Date	Correction Factor*
1	Sept. 18, 1961	.824
2	Sept. 20, 1961	.805
3	Sept. 21, 1961	.796
4	Sept. 22, 1961	.787
5	Sept. 23, 1961	.778
6	Sept. 24, 1961	.769
7	Sept. 25, 1961	.760
8	Sept. 26, 1961	.752
9	Sept. 28, 1961	.734
10	Sept. 29, 1961	.726
11	Sept. 30, 1961	.718

\*Subcritical count rates were divided by correction factor for each day to obtain count rates listed in Table III.

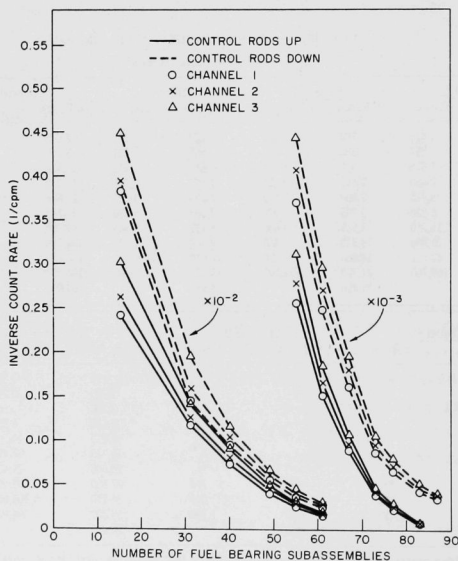


Fig. 9. Approach to Critical - Inverse Count Rate Curves

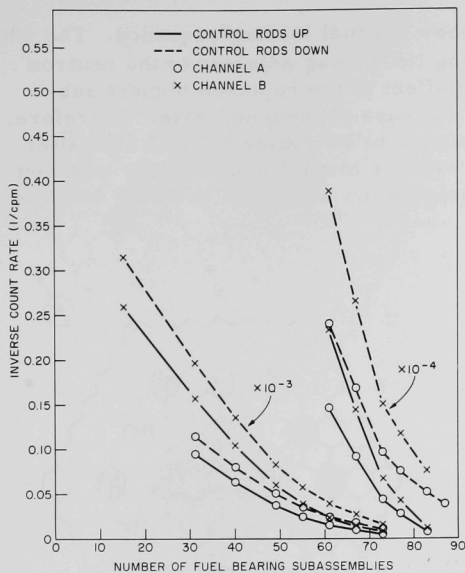
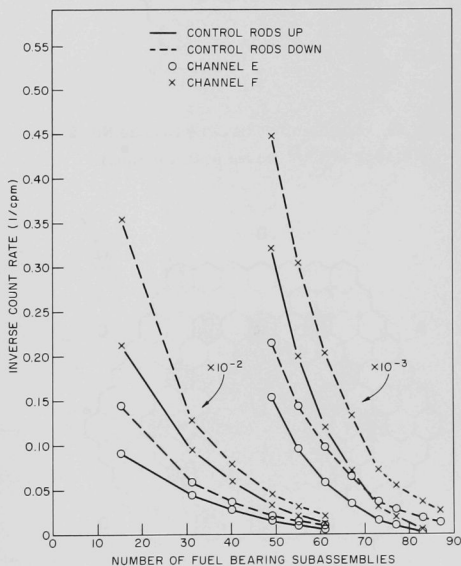


Fig. 10  
Approach to Critical - Inverse  
Count Rate Curves

Fig. 11  
Approach to Critical - Inverse  
Count Rate Curves



Figures 12 through 21 show the fuel loading sequence. The 68th fuel subassembly, the first of Loading No. 8, was adjacent to the neutron source. This removed the shielding effect of the replaced blanket subassembly, resulting in a noticeable increase in the count rate. Therefore, the inverse count rate curve extrapolates to a smaller critical size after Loading No. 8 than the curve would with the blanket subassembly adjacent to the source. A more accurate extrapolation was again possible with the completion of Loading No. 9.

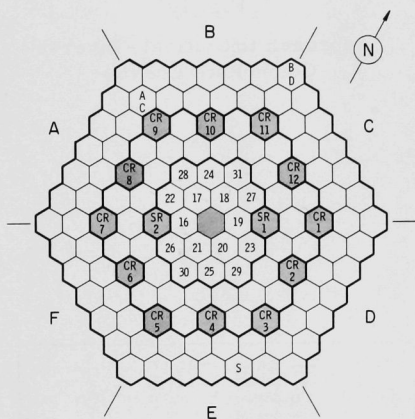


Fig. 12. Approach to Critical - Loading No. 2  
(74.18 kg of  $U^{235}$  loaded on completion)

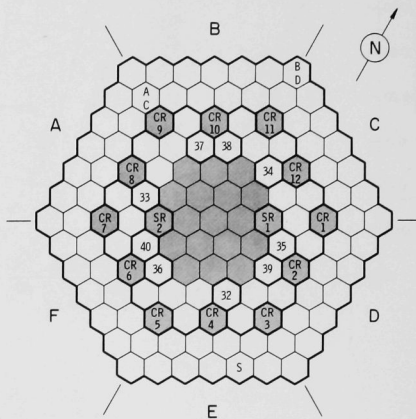


Fig. 13. Approach to Critical - Loading No. 3  
(99.49 kg of  $U^{235}$  loaded on completion)

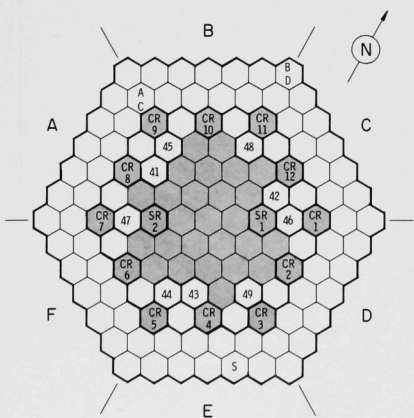


Fig. 14. Approach to Critical - Loading No. 4  
(124.98 kg of  $U^{235}$  loaded on completion)

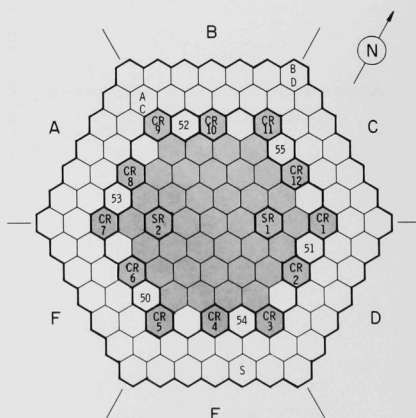


Fig. 15. Approach to Critical - Loading No. 5  
(141.86 kg of  $U^{235}$  loaded on completion)

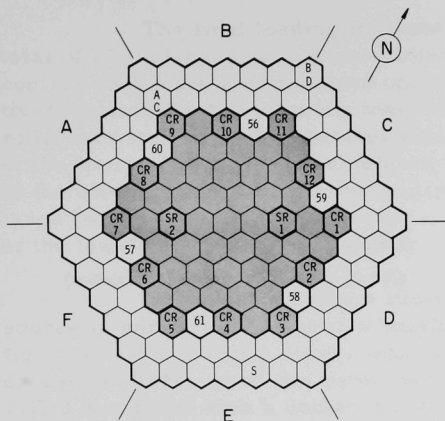


Fig. 17

Approach to Critical - Loading No. 7  
(175.73 kg of  $U^{235}$  loaded on completion)

Fig. 16  
Approach to Critical - Loading No. 6  
(158.81 kg of  $U^{235}$  loaded on completion)

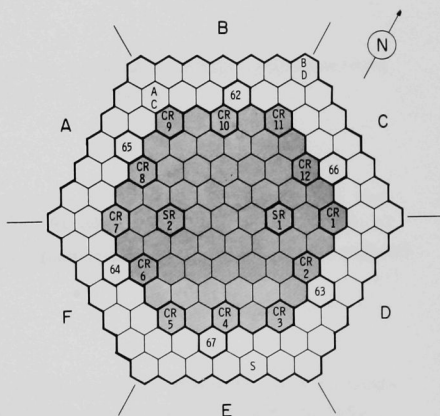
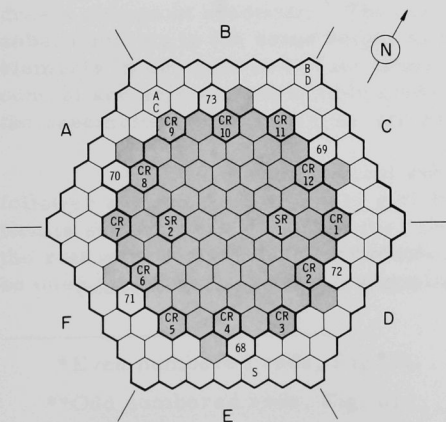


Fig. 18

Approach to Critical - Loading No. 8  
(192.67 kg of  $U^{235}$  loaded on completion)



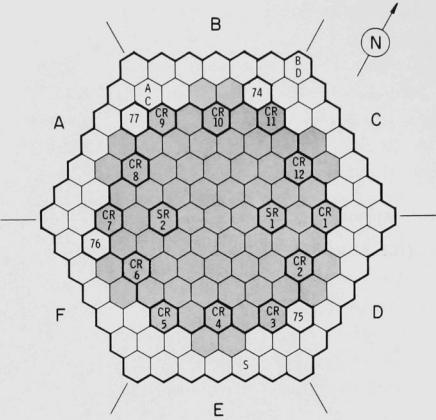


Fig. 19

Approach to Critical - Loading No. 9  
(203.95 kg of  $U^{235}$  loaded on completion)

Fig. 20  
Approach to Critical - Loading No. 10  
(220.88 kg of  $U^{235}$  loaded on completion)

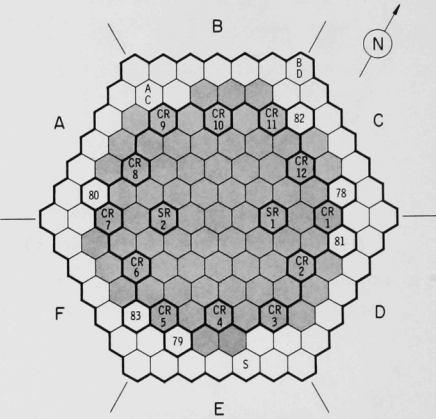
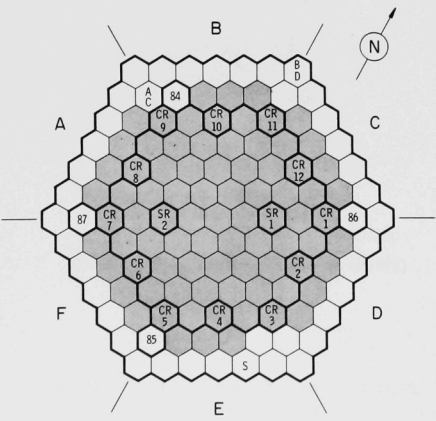


Fig. 21

Approach to Critical - Final Loading No. 11  
(232.18 kg of  $U^{235}$  loaded on completion)





The final loading increment (Loading No. 11, Fig. 21) gave a total of 87 fuel-bearing subassemblies containing 232.18 kg of  $U^{235}$ . The control rods were then inserted one at a time. First, the six more effective\* rods on the "flats" were inserted. Then, the less effective corner\*\* rods were inserted. The reactor diverged on a 100-sec period with eleven of the twelve control rods completely inserted. The exact critical position of the eleventh rod could not be accurately determined at this time. The large (~150 curies) neutron source contributed a large fraction of neutrons at the low Dry Critical power level.

Subsequent loadings replaced the large (~150 curies) neutron source in position 7-E-3 with a small (15 curies) neutron source in position 8-E-5. The small source was also less effective because of the increased distance from the core. Subsequent to source removal, position 7-E-3 was filled with a depleted uranium inner blanket subassembly.

### C. Reactivity Effects

Reactivity effects were measured to evaluate design parameters and to better understand the neutronics of the reactor.

#### (1) Control and Safety Rods

Following the critical approach, the reactivity worths of the control and safety rods were measured. Positive period and subcritical methods were used. Large reactivity worths measured by the subcritical method contain a 10% error.

##### (a) Description of Rods

The control and safety rods in EBR-II move fuel to produce a change in reactivity. The fuel section of the control and safety subassemblies is the same height as the core but contain only 61 fuel elements in contrast to 91 fuel elements in a core subassembly. Each control and safety subassembly contains approximately 1.89 kg of  $U^{235}$  and the assembled rod has a 14-in. stroke.

A special control subassembly was designed with a poison follower section containing 135 g of  $B^{10}$  in boron carbide. This poison section is seven inches above the fuel section so the boron carbide will be in the reactor when the rod is withdrawn. Such a control subassembly could be used to increase the worth of a single control rod.

---

\*Even numbered rods, Fig. 21.

\*\*Odd numbered rods, Fig. 21.

(b) Location of Rods

The number and location of each safety and control rod can be seen in Fig. 22. The two safety rods are in the third row and the twelve control rods are in the fifth row of the core.

(c) Calibration of Control and Safety Rods

After the critical approach, the fuel subassemblies were slightly rearranged to form a more symmetric loading. The large neutron source was replaced with a small antimony-beryllium neutron source which had a strength of 30 curies on August 1, 1961. It had decayed<sup>†</sup> to approximately 15 curies on October 2, 1961, when it was inserted in the reactor. The source location was moved from position 7-E-3 to 8-E-5.

The measured total worths of the control and safety mechanisms are given in Table V. The core loadings were as shown in Figs. 22 and 23. Two slightly different core loadings were used to determine the effect of perturbing the core boundary on the worth of the control rods.

TABLE V. REACTIVITY WORTHS OF CONTROL AND SAFETY RODS

Rod	Core Loading Figure Number	Reactivity Worth	
		Inhours	% $\Delta k/k^{(3)}$
Control Rod*			
No. 10	22	154.0 (1)	0.37
No. 1	22	137.0 (1)	0.33
No. 7 (special)	22	239.0 (2)	0.58
No. 9	22	132.5 (2)	0.32
No. 6	23	163.0 (1)	0.39
No. 2	23	149.5 (1)	0.36
No. 2	23	150.1 (2)	0.36
All 12 Control Rods	22	1854**(2)	4.37
Two Safety Rods	22	430**(2)	1.04
Two Safety Rods	22	425**(2)	1.02

(1) Period Measurement

(2) Subcritical Measurement

(3) 415 inhours = 1%  $\Delta k/k$

\*Even numbered control rods on "flat" of hexagonal core  
Odd numbered control rods on corner of hexagonal core

\*\*Error is  $\pm 10\%$

Control rods No. 1 and 10 were also calibrated over the 14-in. stroke. The calibration curves are shown in Fig. 24.

<sup>†</sup>Sb<sup>124</sup> has a 60-day half-life.

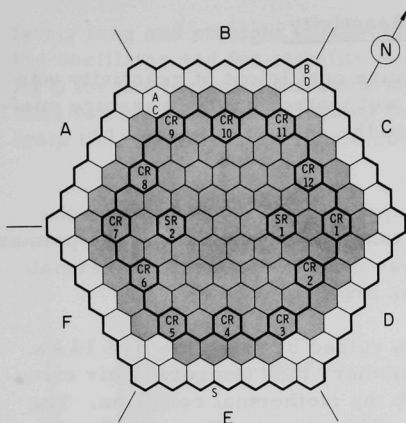


Fig. 22

Core Configuration for Most Control and Safety Rod Measurements  
(Total reactivity worth and incremental calibration; 232.18 kg of  $U^{235}$  loaded into reactor)

Fig. 23

Core Configuration for Reactivity Worth Determination

(Control rods 2 and 6; 235.00 kg of  $U^{235}$  loaded into reactor)

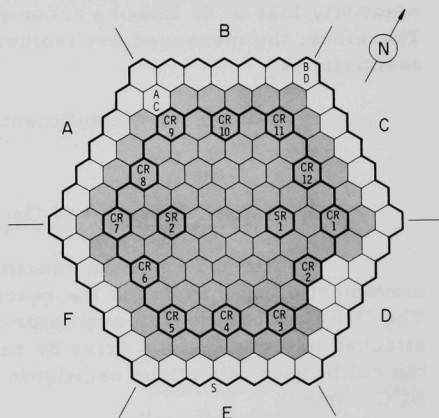
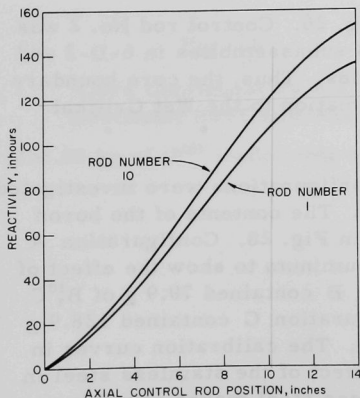


Fig. 24

Control Rod Calibrations



## (2) Temperature Coefficient of Reactivity

The dry isothermal temperature coefficient of reactivity was measured for later comparison with the wet isothermal temperature coefficient. This comparison will help isolate the sodium temperature coefficient of reactivity.

The reactor was cooled by supplying 30° -60°F air from the building air supply through two primary tank viewing nozzles. The primary tank temporary air circulation system was used to establish isothermal conditions. The reactor temperature was lowered to 58°F.

The reactor temperature was raised by using the five 14 kw primary tank immersion heaters. The primary tank temporary air circulation system was again used to establish the isothermal condition. The reactor temperature was raised to 99°F. This gave a  $\Delta T$  of +41°F. A reactivity loss of 25 inhours accompanied the temperature increase. Therefore, the measured dry isothermal temperature coefficient of reactivity is:

$$\begin{aligned}\text{Temperature coefficient} &= -0.6 \text{ Ih}/^{\circ}\text{F} \\ &= -2.6 \times 10^{-5} \Delta k/k/^{\circ}\text{C}\end{aligned}$$

## (3) Static Calibration of Oscillator Rod

The design of the reactor oscillator rod specifies vertical movement of  $B_4^{10}\text{C}$  to obtain the reactivity amplitude for the stability studies. The Dry Critical mockup oscillator rod shown in Fig. 25 was designed to be attached to a control rod drive by replacing the control rod. This enabled the calibration of various oscillator rod configurations which differed in  $B_4^{10}\text{C}$  content.

The reactor was loaded as in Fig. 26. Control rod No. 2 was replaced by the oscillator rod. The two fuel subassemblies in 6-D-3 and 6-D-4 were replaced by blanket subassemblies. Thus, the core boundary near the oscillator rod was a better approximation to the Wet Critical reactor.

Three different oscillator rod configurations were investigated. The calibration curves are shown in Fig. 27. The contents of the boron carbide capsule in cross section are shown in Fig. 28. Configuration A was a reference calibration with 45.7 g of aluminum to show the effect of the stainless steel in the rod. Configuration B contained 70.9 g of  $B_4^{10}\text{C}$  in five  $\frac{1}{4}$ -in.-long annular cylinders. Configuration C contained 128.9 g of  $B_4^{10}\text{C}$  in nine  $\frac{1}{4}$ -in.-long annular cylinders. The calibration curves in Fig. 27 for the two  $B_4^{10}\text{C}$  loadings show the effect of the stainless steel in the rod. The combination of  $B_4^{10}\text{C}$  and stainless steel makes possible a

fairly long and straight portion of the calibration curve over which to move the oscillator rod for stability studies. Figure 29 shows the true worth of  $B_4^{10}C$  for the two configurations as a function of axial position in the core. This is obtained by subtracting the reference (Configuration A) calibration from the two poison bearing measurements (Configurations B and C).

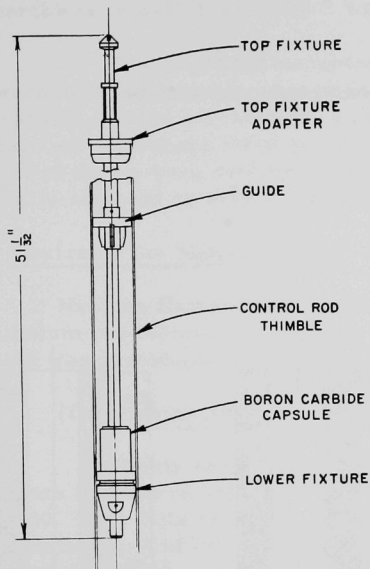


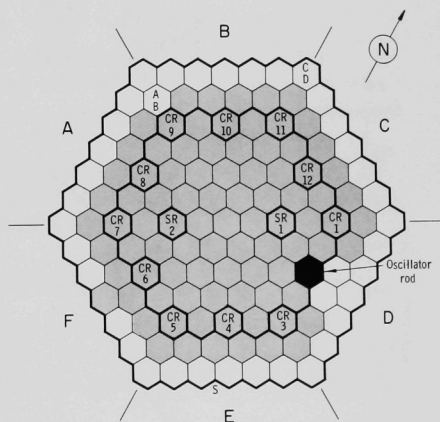
Fig. 25

Dry Critical Oscillator Rod

Fig. 26

Core Configuration for  
Oscillator Rod Calibration

(236.00 kg of  $U^{235}$  loaded into reactor)



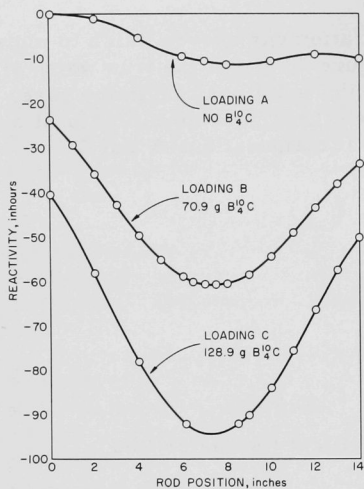


Fig. 27

Oscillator Rod Calibration Curves

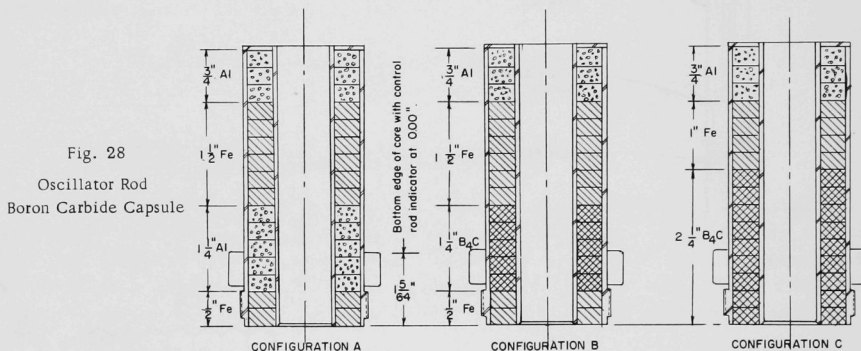


Fig. 28

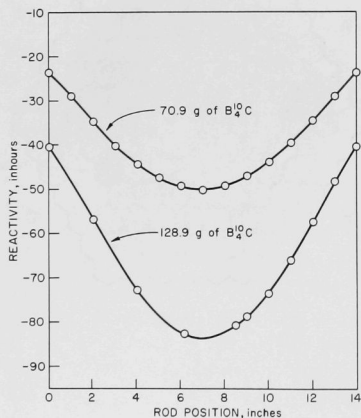
Oscillator Rod  
Boron Carbide Capsule

Fig. 29

Corrected Worth of  $B_4C$  in Oscillator Rod



#### (4) Replacement Worth of Fuel Subassemblies

The reactivity worth of a fuel subassembly when replaced by a blanket subassembly was measured at two different locations. This substitution was made in 6-F-1, a corner of the hexagonal core, and in 6-A-3, the "flat" of the hexagonal core. The replacement worth of the fuel subassemblies in 6-F-1 and 6-A-3 was 115.5 and 161.5 Ih, respectively.

Two fuel subassemblies in 6-D-3 and 6-D-4 were simultaneously interchanged with the blanket subassemblies in 6-C-1 and 6-E-1. The replacement caused a reactivity loss of 103 Ih. This result is essentially consistent with those cited above. The difference must be attributed to the effect of the in-core instrumentation in 7-C-1. The latter location is radially adjacent to 6-C-1 (Fig. 23).

#### D. Neutron Flux Measurements

Neutron flux measurements determined the power distribution and plutonium production in the reflector. The effectiveness of the neutron shield was investigated by measuring the shield leakage flux.

##### (1) Fission and Capture Distributions in the Outer Blanket

Highly enriched ( $\sim 93.2\%$   $U^{235}$ ) uranium and depleted ( $\sim 0.2\%$   $U^{235}$ ) uranium foils were irradiated in three outer blanket positions as shown in Fig. 30. Two foils of highly enriched uranium were placed in position 7-C-4 to monitor each of the three irradiations. The radiochemical analyses of these foils, by R. J. Armani, at Argonne, Ill., are cited in Tables VI, VII, and VIII.

The activity of the fuel alloy was measured following the irradiation of the second set of foils. A 40 watt-hour foil irradiation was completed at 4:19 p.m. on October 11, 1961. On the following day, the fuel subassembly in 6-D-3 was removed from the reactor. At 12:15 p.m. on October 12, 1961, a Juno meter reading indicated that the gamma activity level was 80 mr/hr two inches from the surface of the subassembly at a point opposite the center of the fuel section.

##### (2) Fission Distributions in the Inner Blanket

Depleted and highly enriched uranium foils were irradiated in blanket subassemblies adjacent to the core. These experiments specified the detailed power distribution within a blanket subassembly due to fissions in the foils.

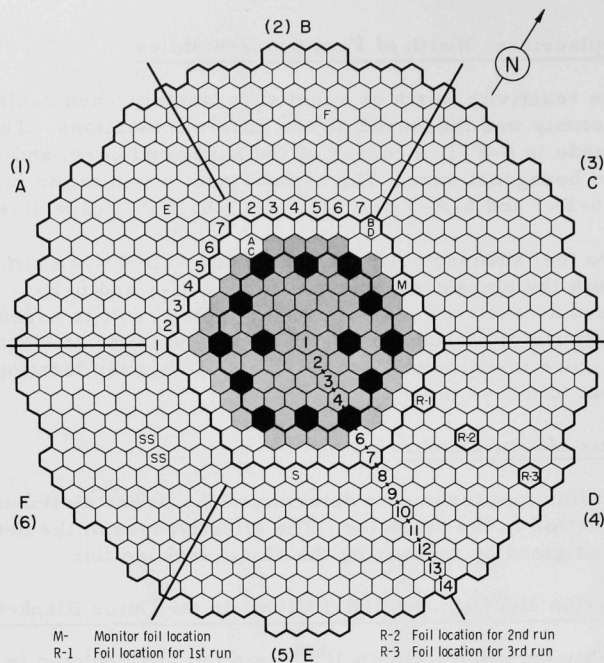


Fig. 30. Foil Locations for Flux Measurements in Outer Blanket  
(232.18 kg of  $U^{235}$  loaded in reactor)

TABLE VII.  $U^{235}$  AND  $U^{238}$  FISSION AND  $U^{238}$  CAPTURE ANALYSIS OF FOIL SET I  
(IRRADIATED IN OUTER BLANKET (10 WATT HOURS))

Radial Location†	Axial Foil Position*	Type of Foil	Foil Number	Foil Wt, g	Total Fissions/g	Error	$U^{238}$ Captures/g	Error
7-C-4**	0	Enriched	4	0.3498	$6.83 \times 10^9$	± 3%		
7-C-4**	0	"	3	0.3386	$6.47 \times 10^9$	± 3%		
8-D-4	29-1/4	"	1E11	4.7400	$4.15 \times 10^8$	± 3%		
8-D-4	10-1/4	"	1E 2	4.6625	$2.29 \times 10^9$	± 3%		
8-D-4	6-1/2	"	1E13	4.5115	$3.15 \times 10^9$	± 3%		
8-D-4	1/2	"	1E15	4.6090	$3.78 \times 10^9$	± 3%		
8-D-4	-7-1/2	"	1E14	4.7082	$2.93 \times 10^9$	± 3%		
8-D-4	-11-1/2	"	1E17	4.6924	$2.21 \times 10^9$	± 3%		
8-D-4	-28-1/4	"	1E12	4.7060	$3.87 \times 10^9$	± 3%		
8-D-4	28-1/4	Depleted	1D68	4.6372	$7.45 \times 10^8$	±15%	$6.32 \times 10^7$	±3%
8-D-4	11-1/4	"	1D67	4.6792	$3.03 \times 10^7$	± 4.5%	$2.35 \times 10^8$	±3%
8-D-4	7-1/2	"	1D48	4.5221	$5.21 \times 10^7$	± 4%	$3.07 \times 10^8$	±3%
8-D-4	-1/2	"	1D69	4.4790	$8.93 \times 10^7$	± 4%	$3.97 \times 10^8$	±3%
8-D-4	-6-1/2	"	1D79	4.4440	$5.85 \times 10^7$	± 4%	$3.29 \times 10^8$	±3%
8-D-4	-10-1/4	"	1D51	4.1447	$3.69 \times 10^7$	± 4.5%	$2.65 \times 10^8$	±3%
8-D-4	-29-1/4	"	1D42	4.5910	$5.33 \times 10^6$	±20%	$5.82 \times 10^7$	±4%

† See Fig. 30.

\*Measured in inches from core midplane; positive values are up, negative are down.

\*\*Monitor Foils.

TABLE VII. U<sup>235</sup> AND U<sup>238</sup> FISSION AND U<sup>238</sup> CAPTURE ANALYSIS OF FOIL SET II  
IRRADIATED IN OUTER BLANKET (~40 WATT HOURS)

Radial Location†	Axial Foil Position*	Type of Foil	Foil Number	Foil Wt, g	Total Fissions/g	Error	U <sup>238</sup> Captures/g	Error
7-C-4**	0	Enriched	13	0.3113	$1.66 \times 10^{10}$	± 3%		
7-C-4**	0	"	14	0.3048	$1.72 \times 10^{10}$	± 3%		
11-D-6	28-1/4	"	1E28	4.7465	$5.35 \times 10^8$	± 3%		
11-D-6	10-1/4	"	1E20	4.7645	$2.08 \times 10^9$	± 3%		
11-D-6	6-1/2	"	1E31	4.7056	$2.53 \times 10^9$	± 3%		
11-D-6	1/2	"	1E21	4.6821	$3.05 \times 10^9$	± 3%		
11-D-6	-7-1/2	"	1E22	4.7287	$2.56 \times 10^9$	± 3%		
11-D-6	-11-1/4	"	1E26	4.6500	$8.36 \times 10^8$	± 3%		
11-D-6	-28-1/4	"	1E23	4.7684	$3.90 \times 10^8$	± 4%		
11-D-6	29-1/4	Depleted	1039	3.9955			$1.16 \times 10^8$	± 3%
11-D-6	11-1/4	"	1027	4.3264	$1.23 \times 10^7$	± 12%	$2.40 \times 10^8$	± 3%
11-D-6	7-1/2	"	1084	4.7815	$1.80 \times 10^7$	± 12%	$2.95 \times 10^8$	± 3%
11-D-6	-1/2	"	1089	4.4830	$2.80 \times 10^7$	± 8%	$3.77 \times 10^8$	± 3%
11-D-6	-6-1/2	"	1078	4.4794	$1.97 \times 10^7$	± 12%	$3.30 \times 10^8$	± 3%
11-D-6	-10-1/4	"	1050	3.7413	$1.61 \times 10^7$	± 10%	$2.63 \times 10^8$	± 3%
11-D-6	-29-1/4	"	1010	4.9243			$7.11 \times 10^7$	± 4%

† See Fig. 30.

\* Measured in inches from core midplane; positive values are up, negative are down.

\*\* Monitor Foils.

TABLE VIII. U<sup>235</sup> AND U<sup>238</sup> FISSION AND U<sup>238</sup> CAPTURE ANALYSIS OF FOIL SET III  
IRRADIATED IN OUTER BLANKET (~167 WATT HOURS)

Radial Location†	Axial Foil Position*	Type of Foil	Foil Number	Foil Wt, g	Total Fissions/g	Error	U <sup>238</sup> Captures/g	Error
7-C-4**	0	Enriched	11	0.3530	$6.28 \times 10^{10}$	± 3%		
7-C-4**	0	"	12	0.3136	$5.74 \times 10^{10}$	± 3%		
15-D-8	28-1/4	"	1E27	4.6488	$1.35 \times 10^9$	± 3%		
15-D-8	10-1/4	"	1E19	4.7266	$1.85 \times 10^9$	± 3%		
15-D-8	6-1/2	"	1E32	4.6815	$2.15 \times 10^9$	± 3%		
15-D-8	1/2	"	1E35	4.5581	$2.49 \times 10^9$	± 3%		
15-D-8	-7-1/2	"	1E42	4.6721	$1.99 \times 10^9$	± 3%		
15-D-8	-11-1/4	"	1E33	4.6699	$1.74 \times 10^9$	± 3%		
15-D-8	-28-1/4	"	1E34	4.5206	$7.06 \times 10^8$	± 3%		
15-D-8	29-1/4	Depleted	10143	4.9963	$4.34 \times 10^6$	± 20%	$2.46 \times 10^8$	± 3%
15-D-8	11-1/4	"	1053	4.9274	$9.58 \times 10^6$	± 12%	$2.00 \times 10^8$	± 3%
15-D-8	7-1/2	"	10128	4.7013	$8.53 \times 10^6$	± 12%	$2.36 \times 10^8$	± 3%
15-D-8	-1/2	"	1035	4.9698	$1.42 \times 10^7$	± 10%	$2.88 \times 10^8$	± 3%
15-D-8	-6-1/2	"	10110	5.0823	$1.11 \times 10^7$	± 12%	$2.36 \times 10^8$	± 3%
15-D-8	-10-1/4	"	10122	4.8766	$1.16 \times 10^7$	± 12%	$2.09 \times 10^8$	± 3%
15-D-8	-29-1/4	"	1023	4.8686	$3.12 \times 10^6$	± 20%	$1.09 \times 10^8$	± 3%

† See Fig. 30.

\* Measured in inches from core midplane; positive values are up, negative are down.

\*\* Monitor Foils.

Figure 31 shows the core configuration for the foil irradiations in 7-C-4 and 7-D-1. Figures 32 and 33 show the relative activation of the highly enriched and depleted uranium foils and also the positions of the foil holders within the special foil bearing blanket subassemblies.

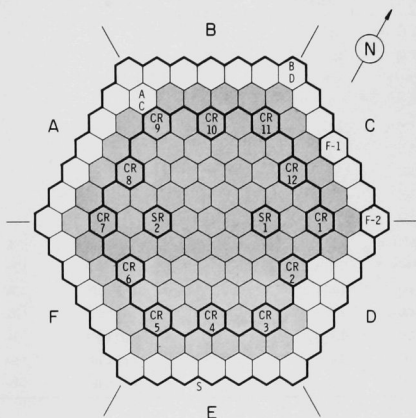


Fig. 31

Core Configuration for Foil Irradiations in 7-C-4 and 7-D-1  
(235.00 kg of  $U^{235}$  loaded in reactor)

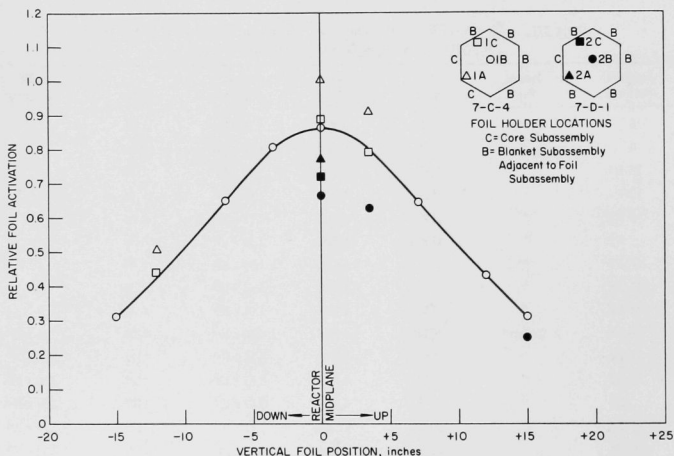


Fig. 32. Highly Enriched Uranium Foil Activations in 7-C-4 and 7-D-1

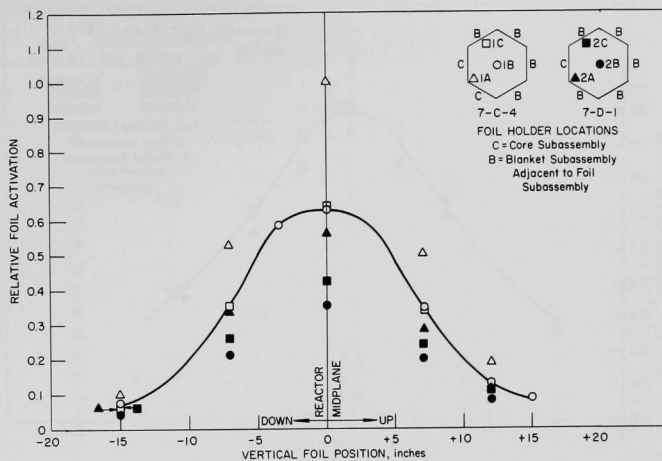


Fig. 33. Depleted Uranium Foil Activations in 7-C-4 and 7-D-1

Figure 34 shows the core configuration for the foil irradiations in 6-C-4 and 7-F-5. The relative foil activations are shown in Figs. 35 and 36. Several foils from 6-C-4 and 7-F-5 were radiochemically analyzed by Armani for both fissions and fertile captures. These results are given in Table IX.

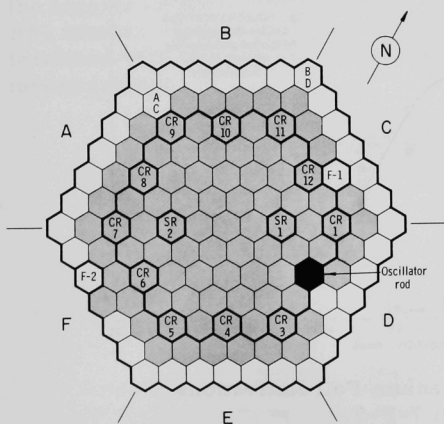


Fig. 34

Core Configuration for Foil Irradiations in 6-C-4 and 7-F-5

(236.00 kg of  $U^{235}$  loaded into reactor)

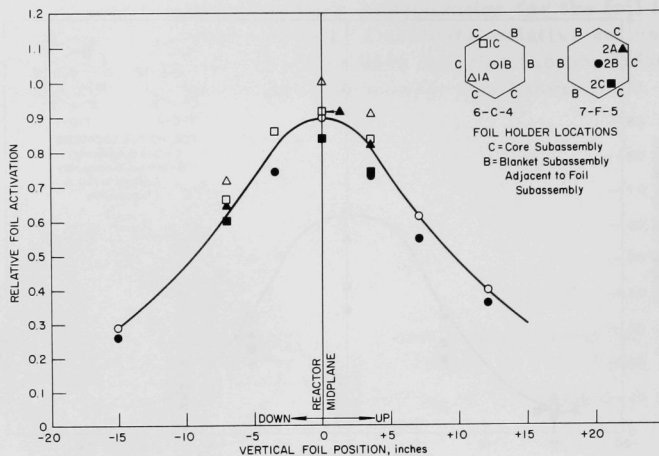


Fig. 35. Highly Enriched Uranium Foil Activations in 6-C-4 and 7-F-5

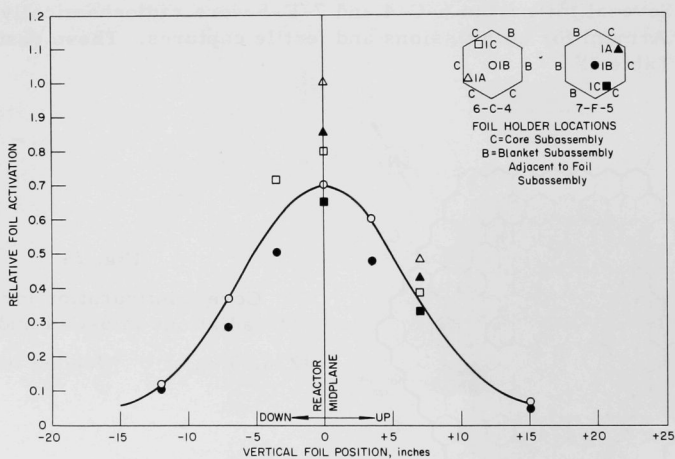


Fig. 36. Depleted Uranium Foil Activations in 6-C-4 and 7-F-5



TABLE IX.  $^{235}\text{U}$  AND  $^{238}\text{U}$  FISSION AND  $^{238}\text{U}$  CAPTURE ANALYSIS OF FOILS IRRADIATED  
IN INNER BLANKET (~80 WATT HOURS)

Subassembly Location	Foil Holder Position†	Vertical Position of Foil, in.*	Type of Foil	Foil Number	Foil wt., g	Total Fissions/g	Error	$^{238}\text{U}$ Captures/g	Error
6-C-4	1A	0	Enriched	E127	.3505	$2.71 \times 10^{10}$	±3%	$1.01 \times 10^8$	±3%
6-C-4	1B	0	"	E133	.3335	$2.38 \times 10^{10}$	±3%	$8.82 \times 10^7$	±3%
6-C-4	1C	0	"	E137	.3395	$2.41 \times 10^{10}$	±3%	$8.87 \times 10^7$	±3%
6-C-4	1B	-3.55	"	E134	.3450	$2.46 \times 10^{10}$	±3%	$8.58 \times 10^7$	±3%
7-F-5	2A	0	"	E141	.3520	$2.42 \times 10^{10}$	±3%	$9.18 \times 10^7$	±3%
7-F-5	2B	0	"	E247	.3515	$2.40 \times 10^{10}$	±3%	$8.93 \times 10^7$	±3%
7-F-5	2C	0	"	E251	.3530	$2.23 \times 10^{10}$	±3%	$8.13 \times 10^7$	±3%
7-F-5	2A	-3.55	"	E142	.3395	$2.52 \times 10^{10}$	±3%	$8.42 \times 10^7$	±3%
6-C-4	1A	0	Depleted	D134	.3580	$1.77 \times 10^9$	±4%	$2.40 \times 10^9$	±3%
6-C-4	1B	0	"	D138	.3770	$1.17 \times 10^9$	±4%	$2.26 \times 10^9$	±3%
6-C-4	1C	0	"	D143	.3475	$1.34 \times 10^9$	±4%	$2.30 \times 10^9$	±3%
6-C-4	1B	-3.55	"	D139	.3485	$1.05 \times 10^9$	±4%	$2.07 \times 10^9$	±3%
7-F-5	2A	0	"	D146	.3790	$1.46 \times 10^9$	±4%	$2.28 \times 10^9$	±3%
7-F-5	2B	0	"	D150	.3730	$1.05 \times 10^9$	±4%	$2.19 \times 10^9$	±3%
7-F-5	2C	0	"	D155	.3780	$1.11 \times 10^9$	±4%	$2.06 \times 10^9$	±3%
7-F-5	2A	-3.55	"	D147	.3815	$1.41 \times 10^9$	±4%	$2.02 \times 10^9$	±3%

† See Fig. 34; 1A and 2A on corner of, 1B and 2B in center of, and 1C and 2C on "flat" of subassembly.

\* Measured from core midplane.

### (3) Leakage Neutron Flux

The effectiveness of the neutron shield was determined by measuring the neutron flux emerging in both the radial and axial directions. High sensitivity [ $\sim 13$  counts/nv(th)]  $\text{BF}_3$  proportional counter response was measured because of the low Dry Critical power level requirement. The total neutron flux is attenuated by 105 from the center of the core to the outside of some shield regions. However, the spectral shift favors  $\text{BF}_3$  counter response. At every position, the counter response was determined with and without a cadmium sleeve. Table X summarizes these investigations.

TABLE X. LEAKAGE NEUTRON FLUX MEASUREMENTS

Counter and Location	Cadmium Cover	Counts/sec/watt	Cd ratio
Counter C behind $J_3$ thimble*	yes	2160	2.94
	no	6355	
Counter E between $J_1$ and $J_2$ thimbles**	yes	651	2.82
	no	1835	
Counter C between $O_2$ and $J_2$ thimbles***	yes	1917	2.28
	no	4375	
Counter E above Na outlet pipe	yes	80	1.86
	no	149	
Counter C on edge of reactor cover	yes	167	1.33
	no	222	
Counter E on center of reactor cover	yes	95	1.50
	no	143	
Inner Shield	Outer Shield	Thimble	
* Graphite	Graphite	Void	
** Void	Graphite	ZrH	
*** Graphite	Borated (3w/o) Graphite	-	

### E. Power Calibration

A power calibration was necessary to prevent overheating the reactor. The high-temperature fission counters (Channels A and B) were calibrated in the Argonne Fast Source Reactor<sup>(5)</sup> prior to being installed in the EBR-II. The calibration was verified by the "absolute" fission counters<sup>(4)</sup> in Channels C and D. Fission counters A and B may be used for power calibration during the Wet Critical Experiments.

A maximum power level of about 150 watts was attained during the Dry Critical Experiments. Most period measurements were made below 20 watts while outer blanket foil irradiations required the higher power (~100 watts) levels.

### F. Determination of Clean Critical Mass

The exact critical mass could be determined after the small neutron source was installed and its position was relocated to the first row of the outer blanket (see Section III-B). The core loading shown in Fig. 22 contained 176.2 inhours of excess reactivity on the basis of the control rod calibrations (Fig. 24) and contained 232.2 kg of  $U^{235}$ . The measured replacement worth of a fuel subassembly, containing 2.81 kg of  $U^{235}$ , was 115.5 inhours. This replacement is for a blanket subassembly in position 6-F-1. Therefore, the fuel worth at the corner of the hexagonal core is 41.1 lh/kg of  $U^{235}$ . The "clean" dry critical mass, with all control rods fully inserted, is 227.9 kg of  $U^{235}$ . The difference between the latter value and the 232.2 kg of  $U^{235}$  actually loaded represents the 176.2 inhours of excess reactivity.

### G. Wet Critical Instrument Configuration

The actual count rates recorded by the  $J_1$  and  $J_2$  thimble fission counters (Tables I and III) suggest that in-core instrumentation will not be required during the Wet Critical approach. This favorable situation greatly simplifies the engineering problems of providing adequate count rates at all times including very low reactor multiplication.

A possible Wet Critical instrument configuration was assembled to conclusively demonstrate that adequate count rates may be obtained without in-core instruments. This investigation also evaluated the use of ZrH to enhance  $J$  thimble instrument response.

These investigations with a substantially subcritical reactor are summarized in Table XI. It may be seen that the presence of ZrH appreciably enhances the thimble fission counter (Channels 1, 2 and 3) response. The factor of five shown on Table XI may be compared with a previously measured factor of three on an aluminum "cooled" EBR-II mockup on ZPR-III.<sup>(3,6)</sup>

TABLE XI. WET CRITICAL INSTRUMENT CONFIGURATION<sup>†</sup>  
 (Reactor  $\sim 6\%$   $\Delta k/k$  Subcritical, neutron source strength  $\sim 70$  curies)

Channel	Thimble <sup>††</sup>	Counter Response (cps)	
		Reference	With ZrH
1	J <sub>1</sub>	22	123
2	J <sub>1</sub>	20	115
3	J <sub>2</sub>	20	105
G*	J <sub>3</sub>	154	-
H*	J <sub>2</sub> **	137	-

<sup>†</sup>In Dry Critical Reactor

<sup>††</sup>See Fig. 5b

\*High sensitivity BF<sub>3</sub> proportional counters

\*\*Above core midplane, all other counters near core midplane

The Wet Critical Experiments will be conducted with the Primary System at 260°C with the interior of the instrument thimbles maintained at 45°C. The presence of rather bulky ZrH appreciably complicates the thimble-cooling problem. Removal of the ZrH and the addition of two high sensitivity [ $\sim 40$  counts/nv(th)] BF<sub>3</sub> startup counters (Channels G and H) reduces the thimble-cooling problem. Furthermore, the BF<sub>3</sub> counters are more sensitive than the fission counters when surrounded by ZrH.

The reference configuration on Table XI provides five counting channels for the Wet Critical Experiment. An overlap factor of seven between the counting rate of the BF<sub>3</sub> and fission counters provides additional assurance for reliable flux monitoring. The absolute counting rates can be adjusted through flexibility in neutron source strength. The provision of two neutron sources whose activity differed by almost a factor of 10 gave such flexibility for the Dry Critical Experiment.

#### IV. SUMMARY

The EBR-II Dry Critical Experiments were conducted in the EBR-II reactor prior to filling the primary system with sodium. All mechanical components and reactor fuel used in these experiments are those that will subsequently be used for normal power operation.

Fuel loading for the critical approach began September 18, 1961. Initial criticality occurred at 7:00 p.m. on September 30, 1961, with a "clean" dry critical mass of 227.9 kg of  $U^{235}$ . This measurement, representing a loading of almost 86 fuel subassemblies, compares favorably with the predicted critical size.<sup>(1,3)</sup> The experimental program was completed on November 1, 1961.

Control rod reactivity worths were measured and the average found to be  $0.37\% \Delta k/k$  as compared to an estimated value of  $0.32\% \Delta k/k$ .<sup>(1)</sup> The two safety rods held a total of  $1.03\% \Delta k/k$  as compared to an estimated worth of  $1.10\% \Delta k/k$ .<sup>(1)</sup>

A determination was made of the dry isothermal temperature coefficient of reactivity, which was found to be  $-2.6 \times 10^{-5} \Delta k/k/^{\circ}C$ . This may be compared with a calculated value of  $-1.8 \times 10^{-5} \Delta k/k/^{\circ}C$ .<sup>(3)</sup>

A calibration of an oscillator rod showed that between 70 and 129 g of  $B_4^{10}C$  will provide adequate reactivity for stability studies in the reactor at power.

Uranium-235 and uranium-238 fission rates were measured in the radial blanket. These measurements were designed to determine precisely the power distribution in the depleted uranium reflector. Some of these measurements determined the over-all power distribution in the reflector, while other measurements enabled a determination of localized variations of power density in the reflector near the core boundary.

Neutron leakage flux from the neutron shield was measured, providing a description of neutron shield effectiveness.

A total of 390 watt-hours was logged on the reactor during the Dry Critical Experiments.

## ACKNOWLEDGMENTS

These experiments represent the combined efforts of many individuals. In particular, the authors wish to acknowledge the indirect efforts of the EBR-II Project Staff who designed the reactor, as well as the EBR-II Operating Staff who did much of the pertinent peripheral work.

## REFERENCES

1. L. J. Koch, et al., EBR-II Dry Critical Experiments, - Experimental Program, Experimental Procedures and Safety Considerations, ANL-6299 (1961).
2. L. J. Koch, et al., Hazards Summary Report - Experimental Breeder Reactor II, ANL-5719 (1957).
3. W. B. Loewenstein, The Physics Design of the EBR-II, ANL-6383 (1961).
4. F. S. Kirn, An Absolute Fission Counter, American Nuclear Society, 2nd Winter Meeting (1957).
5. G. S. Brunson, Design and Hazards Report for the Argonne Fast Source Reactor (AFSR), ANL-6024 (1959).
6. W. P. Keeney and J. K. Long, Idaho Division Summary Report for July, August, September 1960, ANL-6301.





ARGONNE NATIONAL LAB WEST



3 4444 00008102 6

X